

Theoretical and experimental research of six-dimensional force / moment measurement piezoelectric dynamometer

R. Zongjin¹, Danaish¹, Z. Jun¹, X. Tianguo¹ and M.A. Akbar²

¹ School of Mechanical engineering, Dalian University of Technology, Dalian, 116024, China.

Phone: +8615651826700; Fax: +8615651826700

² School of Mechanical engineering, The Hong Kong Polytechnic University, Hong Kong, 999077, China.

ABSTRACT – High-accuracy measurement for force is essential in the Robotics design, Rocket thrust, manufacturing process, and biomedical equipment. To realize the multi-dimensional force/moment measurement, a multi-points force / moment measurement piezoelectric dynamometer capable of measuring spatial force information has been developed. The experimental prototype dynamometer is fabricated according to the designed numerical simulation model (Finite element method: FEM) in which eight three-axis piezoelectric sensors are uniformly distributed in a zigzag pattern. The constructed dynamometer is calibrated both statically and dynamically, static calibration is carried out using a manual hydraulic loader, and the dynamic calibration is performed by impact load technique. The maximum error difference between the theoretical simulations and experimental analyses is approximately 7%. The experimental calibrated results evaluate that the cross-talk error of the applied axile force, normal force and pitch moment is less than 4% and the natural frequency (ω_n) of the dynamometer in each coordinate is greater than 0.35 kHz.

ARTICLE HISTORY

Received: 17th May 2021

Revised: 02nd March 2022

Accepted: 13th May 2022

KEYWORDS

Tri-axial piezoelectric sensors installation

Multi-points force/moment measurement

FEM simulation experiments

Experimental calibration analysis

INTRODUCTION

A six-dimensional force-moment measurement piezoelectric dynamometer is designed and fabricated to measure externally applied load and to collect their six-components force/moment information. The proposed multi-point measurement test system consists of a dynamometer which contains a bottom plate and an upper plate with the installation of eight three-axis piezoelectric sensors, two hydraulic loaders to exert the force/moment manually in X and Z coordinates, two standard force measurement devices, and the main base bed to support the entire dynamometer system. The experimental calibration describes the linearity error, the repeatability error, and the cross-talk error of the fabricated dynamometer. Multi-dimensional measurement models have a great scope in robot designing, NASA satellite, rocket engine thrust testing, aerodynamic force measurement in the wind tunnel, the process of industrial manufacturing and control, biomedical equipment, military equipment, and many other applications [1–4].

In recent years, a lot of research performed on the design of multi-dimensional force-moment sensors, measurement analysis, and fabrication improvement. The designed piezoelectric dynamometer is capable to measure the different load applications to its multi-allocated points in three coordinates. The axile force and normal force maximum up to 12 kN are applied in X- and Z-directions respectively and the pitch moment maximum up to 9.660 kNm is applied along the Y-direction. For the multi-dimensional force-moment measurement, at least three tri-axial piezoelectric sensors are required for measuring the three components of force/moments. This research work is based on using a uniform zigzag shape installation of 8 tri-dimensional piezoelectric load sensors in between the clamped plates of the dynamometer which can measure both the magnitude and direction of the exerted force-moment vectors in spatial direction [5]. The stiffness of the load sensors quartz crystal is high, and therefore, the piezoelectric quartz crystal load sensor has high natural frequency and adequate sensitivity [6]. The environmental temperature may affect the measurement accuracy of the piezoelectric sensor, however, the temperature influence can be minimized by choosing the appropriate piezoelectric material [7]. The eventual aim for the static design of the piezoelectric six-axis force-moment measurement dynamometer is to understand an active design based on its static performance. The mechanical structure, integrated with sensing piezoelectric load cells, and the calibration system is designed to isolate each axis of the designed dynamometer with minimal cross-talk between the various axes [8].

Structural design is particularly important in the design of multi-dimensional force/moment measurement because only with a suitable design, enhancements in its performance can be gained. There are many applications in multi-component force/torque sensors of the parallel mechanisms as it possesses the determined merits of symmetric, compact design and high rigidity. In the static configuration of six components force/torque sensor, active design theory plays an important role, and the static structural/mathematical model functions as its foundation [9]. Design and calibration of multi-component force/torque sensor researched to measure static or dynamic force in multi-directions [10, 11]. The design and validation of a six degree of freedom rocket motor test stand proposed by Z. N. Brimhall [12] and a new six-axis load cell designed by F. Ballo et al., to assess the accuracy and analyze the calibration [13]. Different type of

arrangement patterns of load sensors can be designed to measure the six components of force-moment. In past, many researchers have performed the linearity, repeatability, and cross-talk errors on their designed dynamometer. The below Table 1 includes the various types of piezoelectric sensors arrangements with a different number of sensors installation to measure six DoFs of force-moment.

Table 1. Cross talk error (%) of different arrangements

Authors/Researchers	No. of PE Sensors	Arrangement	DOFs	Cross talk Error (%)
Zhenyuan Jia et al, 2013, [14]	3	Multi-point	6	–
Jia ZY et al, 2010, [15]	6	Hexagonal	6	within 4.5%
Ying-Jun Li et al, 2009, [16]	4	Lozenge	6	>5%
Ying-Jun Li et al, 2009	4	Square	6	<5%
Zhenyuan Jia et al, 2013	4	Square	6	Max 5.3%
Qin lan et al, 2011, [10]	8	Octahedral	6	<4%

PE: piezoelectric; DOF: the degree of freedom.

Piezoelectric materials can find out as natural minerals and also can be produced artificially like; Quartz, Rochelle salt, and ammonium, etc. However, in the studied research, the quartz crystal [17, 18] material is used as piezoelectric material because it has good mechanical strength, resistance to moisture, small dielectric loss, and its properties stable during the change in temperature. Moreover, there are many applications of multi-component force sensors as a novel, robust tri-axial force sensor that has been developed by P. Baki et al., [19] that can be integrated into biomedical and robotic devices. Also, J. A. N. Schleicher discussed the calibration process of a multi-component force/torque transducer as calibration determines the measurement uncertainty [20] and parallel mechanism-based force-torque sensor introduced by T. A. Dwarakanath [21]. Furthermore, M. Kang et al. discussed the design optimization of six-axis force-torque to measure cross-coupling error [22] also M. Gobi presented an error analysis of a new high precision six-axis load cell [23]. Z. G. Zhang et al, have investigated multi piezoelectric effects based on classical piezoelectric theory [24], and the load sharing principle of multi-dimensional force/torque sensor measurement model was researched in reference [25]. Furthermore, Ying-ju Li et al discussed two types of spatial arrangements, lozenge and square arrangements of piezoelectric six-component force/torque sensor in their research [16].

The piezoelectric dynamometer is capable of the measurement of three forces as axial, side/bilateral, normal/vertical forces, as well as three moments as rolling, yawing, and pitching moments of multi-points is designed and is developed. The studied research used an alternate-zigzag shape installation of three-axis piezoelectric load sensors. The multipoint force-moment measurement concept is introduced, contains a numerical simulation carried out using finite element model and the experimental calibration tests are performed. The design of the dynamometer structure is built to analyze the working and measuring principle of the test system and, to represent the multi-allocated force-moment points and a mathematical model is constructed to derive the force-moment equations. The designed piezoelectric dynamometer is verified theoretically by performing the simulation analysis to confirm the safety of the structure. After fabrication, the dynamometer is assembled to record and analyze the experimental performance results. The axile force (F_x), normal force (F_z), and pitch moments (M_y) are exerted to the designed-allocated points in the FEM simulation analysis and in the static calibration experiments. The experimental calibration analysis evaluates that the cross-talk error of the exerted axile load, normal load, and pitch moment is under 4% and, the linearity error is less than 4.5%, and the repeatability error is less than 3%. The analyzed output results of theoretical simulation and experimental measurement analysis should be in agreement and they must show consistency with the applied standard load. The measured theoretical and experimental results of the designed multi-point measurement dynamometer are compared and discussed in detail in section 5.

DESIGN OVERVIEW

The designed dynamometer chooses piezoelectric technology to measure the spatial force-moments. The design of all components is constructed with SolidWorks 2018, and then the designed parts are assembled to construct the piezoelectric dynamometer. The simulation experiments are conducted using FEM on ANSYS 19.2, and calibration experiments are performed after the fabrication.

Three-axis Piezoelectric Sensor

The total height of the installed tri-axial piezoelectric sensor is 12 mm and the length and the breadth are of the same dimension that is 30 mm. The selected single piezoelectric sensor can measure a maximum up to 5 kN force in three coordinates. The piezoelectric sensors output signal in three coordinates as axial force (F_x) in the x-axis, bilateral force (F_y) in the y-axis and normal force (F_z) in the z-axis. The force sensors can respond a signal in the positive as well as in negative directions in all three axes depending on the nature of the exerted load. In Figure 1, the 3D SolidWorks design of the tridimensional piezoelectric sensor with the dimensions and its three coordinates are shown.

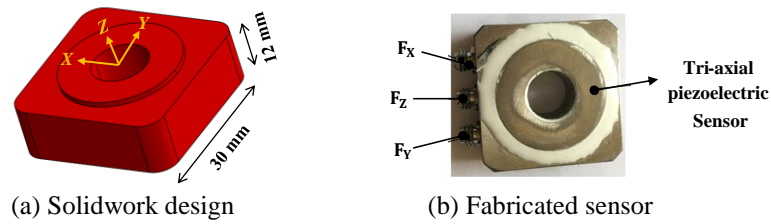


Figure 1. Tri dimensional piezoelectric sensor

Multi-point Piezoelectric Dynamometer Design

The designed piezoelectric dynamometer is capable to measure the three components of force (F_x , F_y and F_z) and three components of moment (M_x , M_y and M_z). Eight three-axis piezoelectric sensors are installed uniformly in zigzag/alternate patterned (see Figure 6) in between the clamped plates of dynamometer. The assembly of the dynamometer system includes a bottom plate, a cover plate, a small support plate, vertical and horizontal hydraulic loaders, and eight symmetrical tri-axial piezoelectric sensors mounted in between clamped plates (Figure 3(a)). Three-axis piezoelectric sensors choose quartz crystal elements based on their quasi-static and dynamic traducer property for force-charge producing. The length, breadth, and height of the entire dynamometer is 3600 mm, 900 mm, and 760 mm respectively (Table 2). The maximum measurement range of the established dynamometer is designed up to 12 kN for axile force in X-direction and normal force in Z-direction and 9.66 kNm for pitch moment along Y-axis. The SolidWorks design of the experimental model with six-components of force/moment is shown in (Figure 2) and the structural parameters and mechanical properties of the designed parts are listed in Table 2.

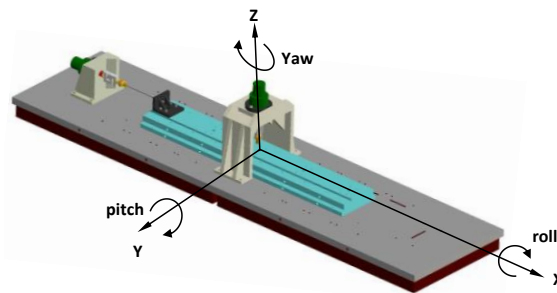


Figure 2. Six-components of the piezoelectric dynamometer (rotation axis definition)

In the theoretical and experimental platform setup, the arrangement mode of the load sensors installation is flexible as there is a maximum of sixteen slots for sensors installation; however, the designed dynamometer choses eight three-axis piezoelectric sensors housing in zigzag/alternate shape. The designed alternate/zigzag patterned arrangement offers easiness in housing the three-axis piezoelectric sensors and to perform the FEM simulations and calibration experiments. Creating an improved and flexible arrangement pattern installation of load sensors result, less cross-talk error, and provide effective measurement results.

Table 2. Main structural parameters of multi-point force/moment measurement dynamometer

Component's Name	Length (mm)	Width (mm)	Height (mm)	Material	Poisson's ratio (pa)	Elastic modulus (pa)	Density (Kg/m^3)
Base support bed	3600	900	150	C45	0.3	2^{11}	7850
lower plate	1800	340	29	C45	0.3	2^{11}	7850
upper plate	1800	300	55	C45	0.3	2^{11}	7850
Three-axis piezoelectric sensors	30	30	12	304	0.3	2^{11}	7850
Small support plate	150	150	100	C45	0.3	2^{11}	7850
Preload fixing bolts	75	M10	-	304	0.3	2^{11}	7850
Hydraulic (F/M) loader (V)	248	600	610	C45	0.3	2^{11}	7850
Hydraulic (F/M) station (H)	304	324	246	C45	0.3	2^{11}	7850

The three-axis sensors are assembled in between the clamped plates and a pre-tightening force has been applied during the bolting. While designing the model, it has been noticed that direct fixation of sensors in between the upper and lower

plates can result in some assembly errors which can affect the measurement accuracy results. Therefore, to reduce the installation error of piezoelectric sensors, the square slots (30x30 mm) with 1 mm height are constructed on the lower and upper both plates (see empty slots in Figure 6).

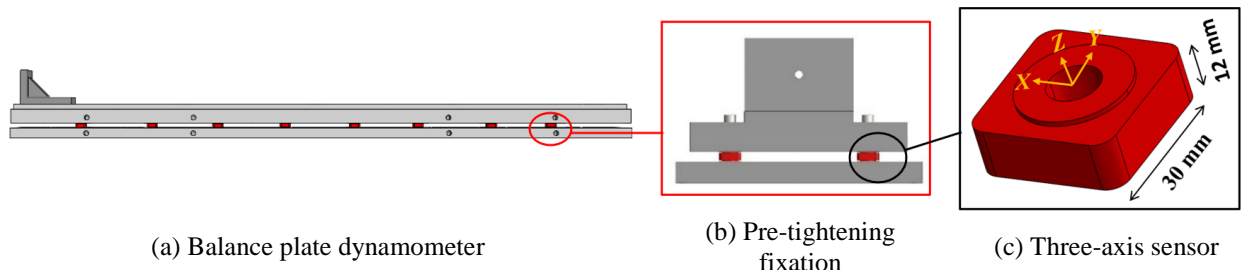


Figure 3. Assembly of three-axis piezoelectric sensors

The dynamometer assembly includes four main parts as, a cover plate, a bottom plate, eight pre-tightening bolts, and eight three-axis piezoelectric sensors. The horizontal distance and perpendicular distance in between the slots for sensors installation are 400 mm and 190 mm respectively. The three views of the multi-dimensional piezoelectric dynamometer model are shown in Figure 4. The bottom and cover plate consist of 2 parallel lines for sensor mounting. The holes/slots for the sensor installation are designed in such a way that the theoretical and experimental measurements of multi-points force/moment is possible by using either any combination/arrangement pattern of three-axis piezoelectric sensors. The model includes two manual hydraulic load stations in the design one is a vertical hydraulic loader (can easily move parallel to the base plate) which is installed to the top of dynamometer to apply the force in Z-direction and moment along the Y-axis and another one is a horizontal hydraulic loader (cannot move) which is fixed at the end of the balance plate to apply the axile force in X-direction (see Figure 14).

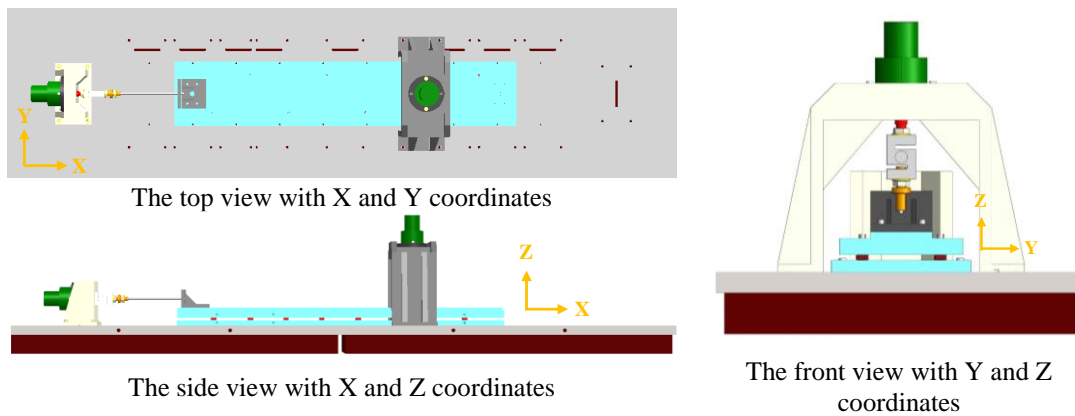


Figure 4. Three views of alternate/zigzag patterned piezoelectric dynamometer

STRUCTURAL MODEL AND MEASUREMENT PRINCIPLE

A structural diagram of the dynamometer is constructed to highlight the three-axis output of the installed piezoelectric force sensors, to present the allocated positions for the designed standard loads and to show the marked points for load application. The measurement principle of the designed dynamometer mainly describes the piezoelectric sensors' measurement technology and their zigzag patterned installation. Furthermore, a mathematical model is developed and equations are derived to measure the total generated force/moment.

Model Structure

The three coordinates of the piezoelectric dynamometer are highlighted, and the main dimensions are constructed. The three force components in x, y, and z directions can be measure with a single three-axis piezoelectric sensor. However, the single sensor is not enough for measuring the three moment components such as pitching, yawing and rolling. Therefore, at least three piezoelectric sensors with a uniform or zigzag/alternate pattern arrangement can be designed and implemented to measure the six-dimensional force-moment. The constructed structural diagram describes the assigned multi-points for load application and presents the three-axis output to the mounted load cells. Where S1-S8 are the installed piezoelectric sensors and P1-P6 are the allocated multi-points to apply the intended range of force-moment (see Figure 5 below).

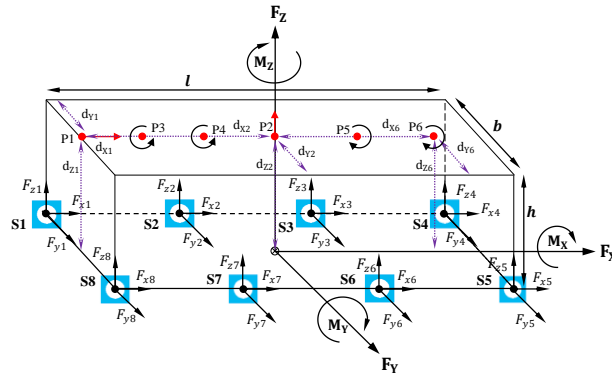


Figure 5. Structural measurement diagram of piezoelectric dynamometer

Where, d_{xj} , d_{yj} , and d_{zj} are three coordinated distances of the marked load points (P1-P6) where $j=1,2,3,\dots,6$, and F_{xi} , F_{yi} and F_{zi} is the output response of piezoelectric sensors where ‘i’ represents the number of corresponding load sensors. The designed distances of the located points in the Y-direction is symmetrical i.e., $d_{y1}-d_{y6}=170\text{ mm}$ and, the vertical distance in the Z-direction i.e., $d_{z2}-d_{z6}=55\text{ mm}$, except the P1 which has $d_{z1}=105\text{ mm}$. Each point P₁-P₅ is designed with a constant distance of $d_{x1}-d_{x5}=402.5\text{ mm}$ in the axial direction except for the P1. The length of the structural diagram of diagonal pattern installation is $l=1800\text{ mm}$, width is $b=390\text{ mm}$, and height is $h=96\text{ mm}$. The horizontal and vertical distance between the slots for sensors housing is 400 mm and 390 m respectively. The six force/moment components of the dynamometer are shown, and the position of applied load is mentioned in the structural design.

Measurement Principle

The developed dynamometer chooses the tri-axial piezoelectric sensing technique is primarily foundation on its several advantages [26] such as good stability, good static rigidity, high natural frequency, high sensitivity, and good frequency response [27]. Measurement principle consists of eight tri-axial piezoelectric sensors that are fixed in between mounted plates to measure the six components of force/moment. The tri-dimensional sensors are mounted in the zigzag/alternate patterned combination (see Figure 6). When the spatial forces act on the tri-axial piezoelectric sensors, the load cells response the electric charge signal in three coordinates as F_{xi} , F_{yi} and F_{zi} (see Figure 5). The measured voltage output of installed load cells is recorded to calculate the multi-points force/moment. The dynamometer response output is F_x , F_y , F_z are the drag, side and lift forces and M_x , M_y and M_z are rolling, pitching and yawing moments. The performance capability of the piezoelectric force sensors can be assured by comparing the measured results with applied standard loads.

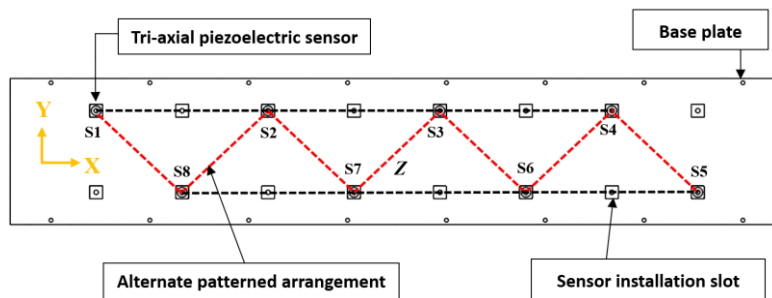


Figure 6. The zigzag/alternate patterned installation

Six points are assigned to exert the designed load ranges of axle force ‘ F_x ’ in X-axis and normal force ‘ F_z ’ in Z-axis, and pitch moments ‘ M_y ’ along Y-axis. A single point named as P1 is allocated at the end of the dynamometer plate with an axial distance $d_{x1}=900\text{ mm}$ from the center of the dynamometer plate for the axle force. The point P2 is marked on the center of the cover plate to apply the central normal force in the Z-axis. And the other four points named as P3, P4, P5, and P6 are allocated on the left (for the clockwise moment) and right (for anti-clockwise moment) side to the center of the cover plate to apply the pitch moments along the Y-axis.

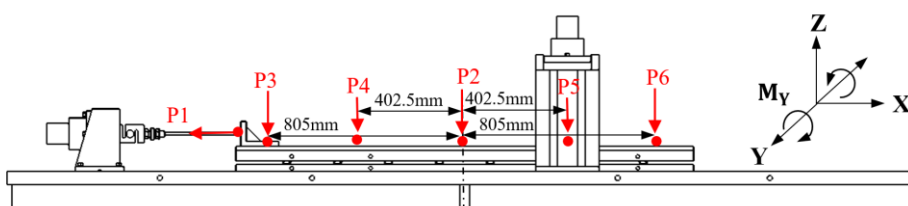


Figure 7. Schematic diagram of multi-points (F/M) piezoelectric dynamometer

Mathematical Model

The mathematical model is evaluated to derive the force and moment equations in three-dimensions. Therefore, it is essential to know the exact locations and output of each sensor for easily computing and analyzing the data. The symbol ‘ l_i ’ represents the horizontal distance between mounted sensors in X-direction ‘where ‘ l ’ defines the length in between two symmetrical positioned sensors and ‘ i ’ is $n=1,2,3,4$ (Figure 8).

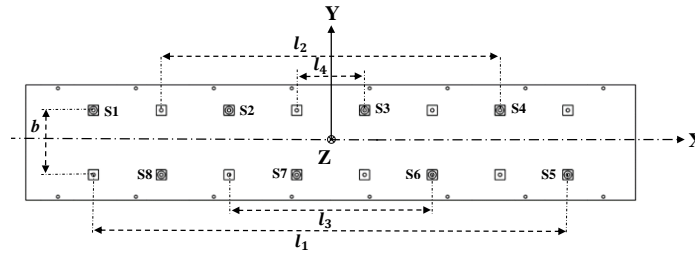


Figure 8. 2D diagram of the mathematical model

The general formula can be used for measuring force and moment;

$$F = F_x + F_y + F_z \tag{1}$$

$$M(F) = M_x + M_y + M_z \tag{2}$$

The three forces can be expressed as;

$$F_x = \sum_{i=1}^n F_{xi} \tag{3}$$

$$F_y = \sum_{i=1}^n F_{yi} \tag{4}$$

$$F_z = \sum_{i=1}^n F_{zi} \tag{5}$$

The force can be computed directly by summing the output of all sensors in the symmetric direction. But, the three-moments of the alternate/zigzag arrangement can be stated as;

$$M_x = k_{Mx} \frac{(F_{z1} + F_{z2} + F_{z3} + F_{z4} - F_{z5} - F_{z6} - F_{z7} - F_{z8})b}{2} \tag{6}$$

$$M_y = k_{My} \frac{(F_{z5} - F_{z1})l_1 + (F_{z4} - F_{z8})l_2 + (F_{z6} - F_{z2})l_3 + (F_{z3} - F_{z7})l_4}{2} \tag{7}$$

$$M_z = k_{Mz} \left(\frac{(F_{x5} + F_{x6} + F_{x7} + F_{x8} - F_{x1} - F_{x2} - F_{x3} - F_{x4})b + (F_{y5} - F_{y1})l_1}{2} + \frac{(F_{y4} - F_{y8})l_2 + (F_{y6} - F_{y2})l_3 + (F_{y3} - F_{y7})l_4}{2} \right) \tag{8}$$

Where F_{xi} , F_{yi} , F_{zi} ($i=1,2,3,\dots,n$) as expressed in Eqs. (3), (4) and (5) are the axial, lateral and vertical forces and M_x , M_y and M_z as expressed in Eqs. (6), (7) and (8) are roll, pitch, and yaw moments of the dynamometer. The parameters k_{Mx} , k_{My} and k_{Mz} are the correction factors and can be concluded in the calibration (the correction factors are related to the errors of the mechanical machining, experimental equipment, or the assembly of the model).

NUMERICAL MODEL (FINITE ELEMENT ANALYSIS FEA (SIMULATION))

ANSYS 19.2 software is used for theoretical simulation analysis. The CAD design of the dynamometer is imported and mesh properties are set up. The model is meshed into 166205 elements and 286066 nodes. FEM simulation experiment is conducted to measure the force reactant outputs of the installed sensors with multi-points load allocation.

The unidirectional force maximum up to 12 kN is applied in axial-direction and normal-direction, and clockwise and anti-clockwise pitch moment maximum of 9.66 kNm is applied along Y-axis (see Figure 7).

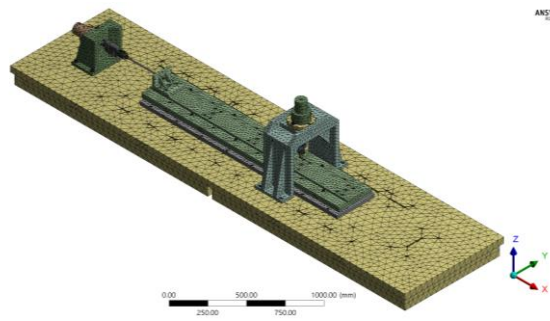
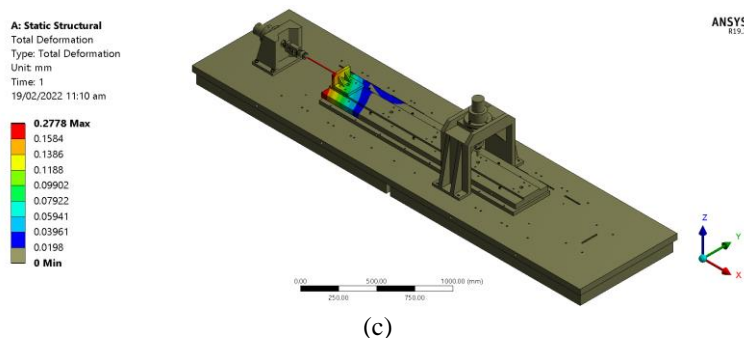
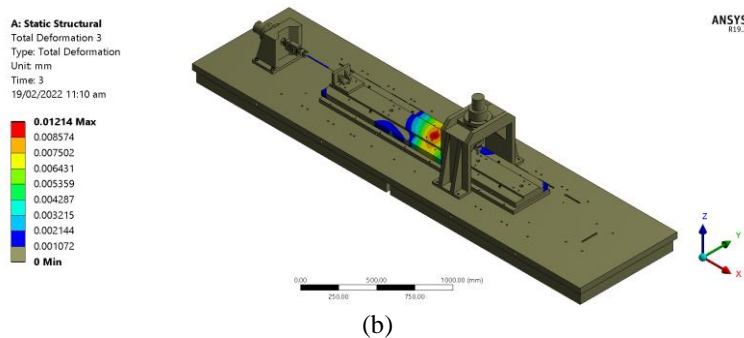
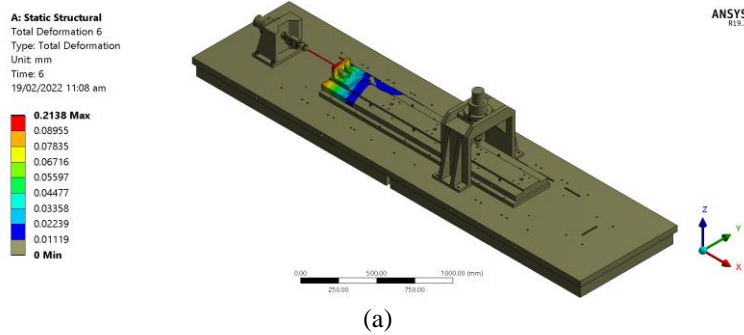


Figure 9. The generated mesh and three coordinates of multi-points piezoelectric dynamometer

Stress and deformation analysis

Figure 10 and Figure 11 illustrate the total deformation and equivalent stress analyses respectively when a force maximum of $F=12$ kN and a moment maximum of $M=9.66$ kNm is applied to the allocated points in defined directions. The numerical model is suitable to apply either the positive or negative force/moment. The force can be applied as compression or as the pulling force and the moment can be applied as clock-wise or anti-clockwise. However, in FEM simulation analysis a single force has been applied in the X-axis as tension force and the Z-axis as compression force and is considered as negative and positive respectively. The clockwise and anti-clockwise moment is applied along the Y-axis and is also considered as positive and negative respectively.



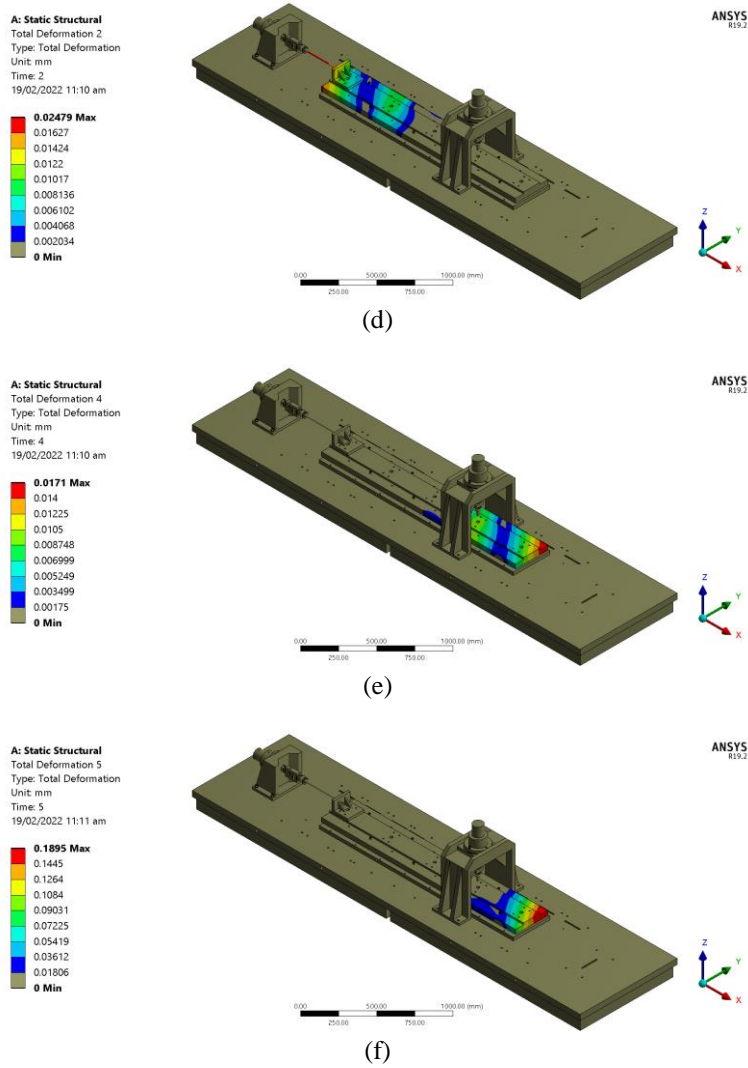
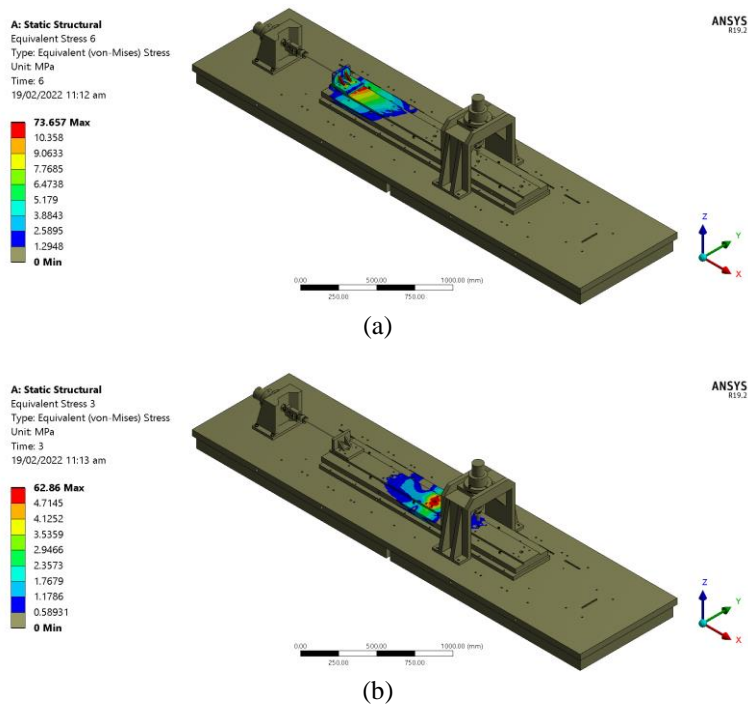


Figure 10. FEM simulation (total deformation) of the axile force, normal force, and pitch moments; (a) axile force (F_x) on P1, (b) normal force (F_z) on P2, (c) anti-clockwise pitch moment (M_{y1}) on P3, (d) anti-clockwise pitch moment (M_{y2}) on P4, (e) clockwise pitch moment (M_{y3}) on P5, (f) clockwise pitch moment (M_{y4}) on P6



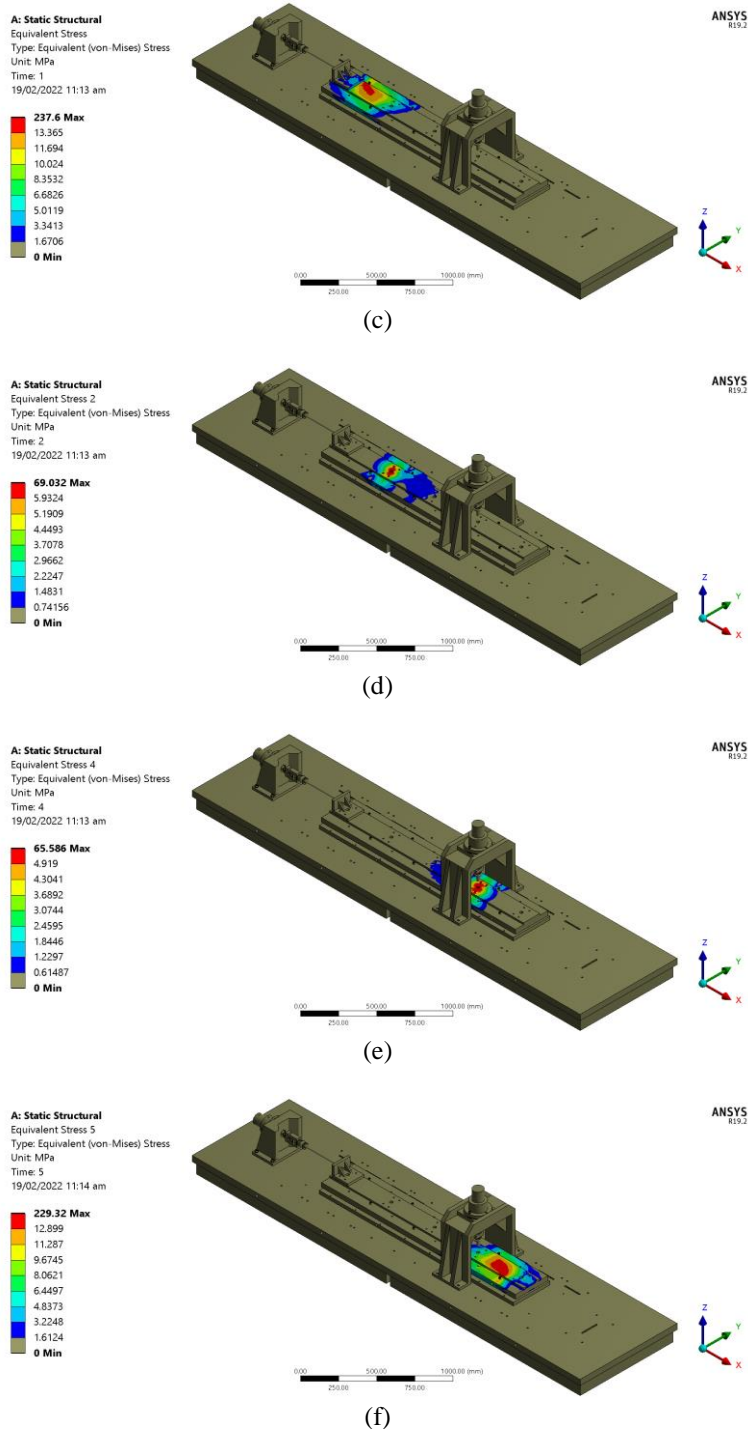


Figure 11. FEM simulation analysis (equivalent stress) of the axle force, normal force and pitch-moments; (a) axle force (F_x) on P1, (b) normal force (F_z) on P2, (c) anti-clockwise pitch moment (M_{Y1}) on P3, (d) anti-clockwise pitch moment (M_{Y2}) on P4, (e) clockwise pitch moment (M_{Y3}) on P5, (f) clockwise pitch moment (M_{Y4}) on P6

FEM model is developed to apply the vertical load, axle load, and moment load, and stresses under each single force/moment are calculated by FEM simulation as shown in Figure 11. The located position of applied force/moment are shown in Figure 7, and the amount of input force and moment to the elastic body is listed in Table.3. The stress outputs under the applied normal force F_z is found lower than the exerted axle force F_x and their maximum equivalent stress is calculated 63 MPa and 74 MPa respectively (see Figure 11(b) and Figure 11(a)). Whereas the stress analysis outputs of moment loads is found maximum of 237 MPa and 229 MPa of moment M_{Y1} and M_{Y4} respectively. The stress analysis values of the other two moment load points (i.e., M_{Y2} , M_{Y3}) are within 70 MPa (see Figure 11(d) and Figure 11(e)). The maximum stresses all occur on or near the located points of applied force/moment. These results of the finite element model analysis demonstrate that the maximum stress under each force/moment of the dynamometer structure is less than its allowable stress. The maximum deformation value is found approximately $\delta = 0.28$ mm at P3 of the pitch moment as

shown in Figure 10(c) The simulation analysis of equivalent stress and total deformation in the axle, normal, and pitch moment direction are acceptable for the safety of the designed piezoelectric dynamometer.

Table 3. FEM simulation experiments of piezoelectric dynamometer

Applied load		Measured force/moment (N/Nm)					
Force (kN)	Moment (kNm)	F_x	F_y	F_z	M_x	M_y	M_z
$F_x = -12$ kN	$M_{y5} = -1.332$ kNm	-11995.60	0.00	0.01	21.54	-1314.08	2.46
$F_z = 12$ kN	0	0.00	0.00	11996.62	0.03	0.00	0.24
$F_{z1} = 12$ kN	$M_{y1} = -9.66$ kNm	0.03	0.02	11999.83	-53.67	-9607.70	-6.91
$F_{z2} = 12$ kN	$M_{y2} = -4.83$ kNm	0.06	0.01	11999.81	-4.77	-4834.55	-0.53
$F_{z3} = 12$ kN	$M_{y3} = 4.83$ kNm	0.04	0.01	11999.85	4.65	4834.36	0.48
$F_{z4} = 12$ kN	$M_{y4} = 9.66$ kNm	0.04	0.05	11999.46	53.29	9611.20	6.95

The designed modeling method and static load technique are used in the theoretical model (FEA; finite element analysis) to evaluate the safety and to verify the effectiveness of the developed design subjected to multi-points loading. The maximum error value up to 0.54 percent is found, when pitch moment is applied in anti-clockwise direction on P3 and in the clockwise direction on P6 as shown in the 3rd and last row of the 6th column in Table 3. The simulation measured results are approximately are in the ranges from 98.5% to 100% of the employed axle force, normal force, and pitch moments. The theoretical measured results proved that the designed dynamometer can measure the multi-points load in X- and Z-directions accurately. The FEM simulation analysis results are quite good as the simulation results of the FEM model agree with the exerted standard force/moment which verifies the safety and measurement accuracy of the designed dynamometer.

CALIBRATION EXPERIMENT SYSTEM RESULTS

The experimental platform of three-axis piezoelectric sensors and dynamometer is defined, and the diagram of the experimental setup process is drawn to understand the calibration methodology of the designed multi-points measurement system. The static calibration and dynamic calibration are performed, and the analyzed results are discussed.

Experimental Calibration Work

Multi-points (F/M) measurement piezoelectric dynamometer demonstrated and assembled to perform the calibration experiment, and the schematic diagram is drawn according to the operating and measuring principle [28] of the designed dynamometer. The efficiency and quality of the piezoelectric dynamometer calibration directly depend on the performance of the platform, and the work status of the test system can be simulated [29, 30]. Therefore, in experimental calibration, the characteristics of piezoelectric cells are carried out individually, and each force sensor is calibrated before the installation (see Figure 12). Calibration is a method that verifies the relationship between the known standard input force/moment and the measured output of the sensors/dynamometer. The calibration of the tri-axial piezoelectric sensors is an important component in the design of the dynamometer, as the calibration result of the experimental system can directly affect by the use of calibrated load sensors.

A preload of 15 kN is applied during the static calibration of tri-axial piezoelectric sensors. A single force maximum up to 100 N, 1000 N, and 2000 N is used in X, Y, and Z-directions during calibration experiments of load sensors (Figure 12). The calibrated data is recorded for every 10 N in X-axis, for every 100 N in Y-axis, and every 200 N in Z-axis. The calibration step is repeated five times to calculate the calibration output error of each sensor (see Table 4). Then good result sensors are selected to house in the main dynamometer to conduct the calibration experiment.

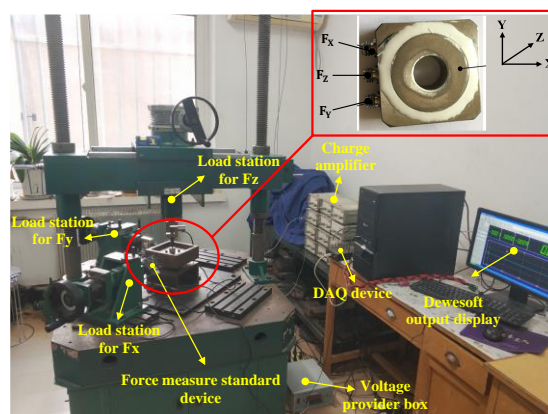


Figure 12. Calibration diagram of the three-axis piezoelectric sensor

The output charge ranges for sensors calibration are set differently in each direction as in the X-direction and Y-direction 1 N is set equal to 1 V and in Z-direction 1N is set equal to 0.1 V. The calibration experiment is conducted in the lab and the calibrated data is analyzed for all eight sensors, and their linearity error (%), repeatability (%) and sensitivity (pC/N) values are shown in below Table 4.

Table 4. Static calibration of eight tri-axial piezoelectric sensors

Co-ordinates Sensor No.s	Linearity error (%)			Repeatability error (%)			Sensitivity (pC/N)		
	X	Y	Z	X	Y	Z	X	Y	Z
Sensor.1	0.125	1.098	0.529	0.258	0.914	2.01	8.057	7.905	3.776
Sensor.2	1.248	0.389	0.12	0.268	0.767	0.195	7.703	7.649	3.82
Sensor.3	0.291	0.189	0.704	1.175	0.372	0.347	7.338	7.419	3.7
Sensor.4	0.217	0.505	0.161	0.465	0.790	0.248	7.814	7.5	3.568
Sensor.5	1.187	0.543	0.203	1.482	0.184	0.398	7.876	8.082	3.8
Sensor.6	0.082	0.261	0.183	0.695	0.975	0.192	7.646	7.958	3.78
Sensor.7	0.519	0.575	0.101	1.64	0.745	0.578	8.353	8.24	4.358
Sensor.8	0.203	0.536	0.082	1.638	0.629	0.164	7.571	7.72	3.648

Many factors influence the accuracy of piezoelectric sensors such as piezoelectric coupling error, sensors assembly error during calibration, and random gross error. As Jun zhang et al discussed the influence of assembly error of sensor on the test accuracy of three-axis force unit can not be avoided [31]. Therefore, because of the various factors the error in some cases increases, however the measured calibration results of all eight sensors are acceptable (see Table 4), and these sensors are used in the piezoelectric dynamometer.

Figure 13 highlights the experimental process set up; at the first step, A pre-tightening load of 15 kN is applied during bolting of the calibrated piezoelectric sensors in an established zigzag pattern. The static calibration process began with the characterization of each point load on the balance plate using manual hydraulic force load to measure the output results of the various components of force/moment. The experimental work diagram of the static calibration, including the vertical and horizontal hydraulic load sets which are fixed with the simulation device. The standard force measurement device (MCL-S2 36711) has a maximum capacity $F_{max}=30$ kN is equipped in horizontal and vertical hydraulic loaders to measure the actual standard applied loads (Figure 14). Each piezoelectric sensor's output wires are connected to a charge amplifier (Kistler). Then the data acquisition card (DT9834) with a maximum of 16 channels is connected to transmit the output information to the host computer, and the measured results are recorded using deweSoft software during calibration.

The schematic diagram of Calibration methodology (Figure 13) describes the relationship of applied standard force (N) on allocated points and output of measured charge (V) converted in steady force (kN) in three coordinates. The applied standard force ranges from 0 to 12 kN, and the calculated output Charge ranges from 0 V to <13.5 V. In experimental calibration the output Charge ranges are set as; 1 N is equal to 0.001 V for each coordinates X, Y, and Z-directions.

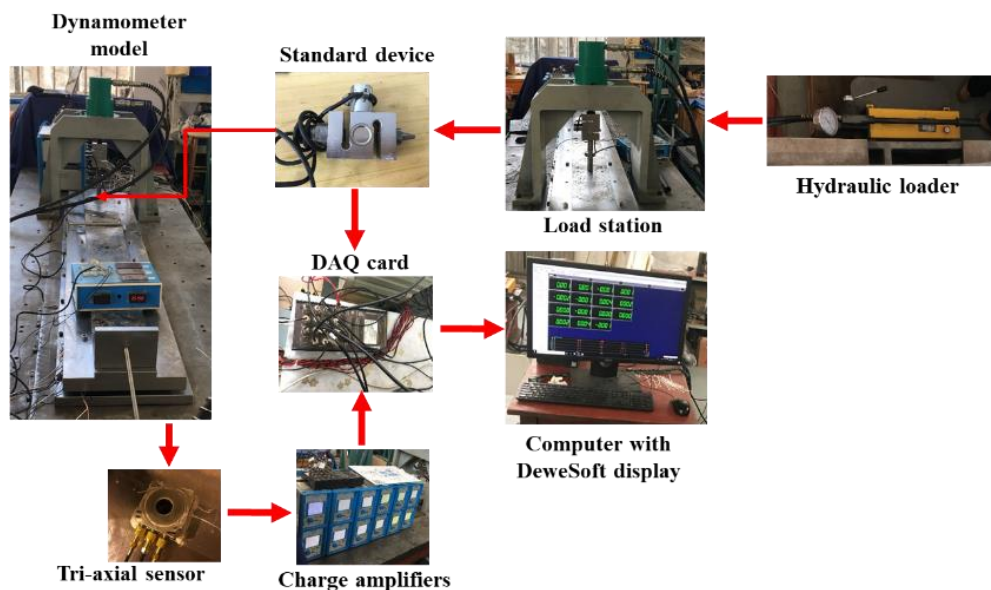


Figure 13. Schematic diagram of calibration methodology and experimental setup of the dynamometer test system

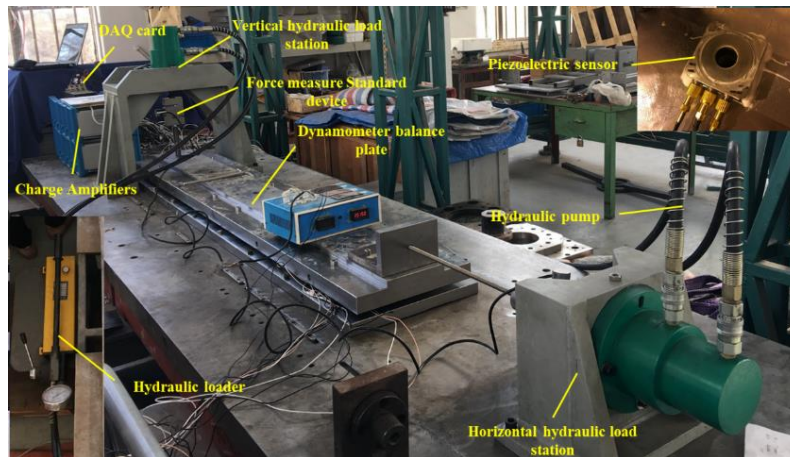


Figure 14. Assembled multi-points force/moment measurement piezoelectric dynamometer

Static calibration experiment

The test system is ready to conduct the static calibration, and experimental static calibration of multi-points force/moment dynamometer is shown (Figure 14). The calibration experiments for a single force maximum up to 12 kN is applied in X-direction and Z-direction for every 3 N, and a single moment maximum up to 9.66 kNm is applied along Y-axis for every 2.415 kNm. The experiment is repeated for 3 times to calculate the average output signal and to find the parameters that affect the performance and the measuring accuracy of the piezoelectric dynamometer.

Static analysis of axle force in X-direction

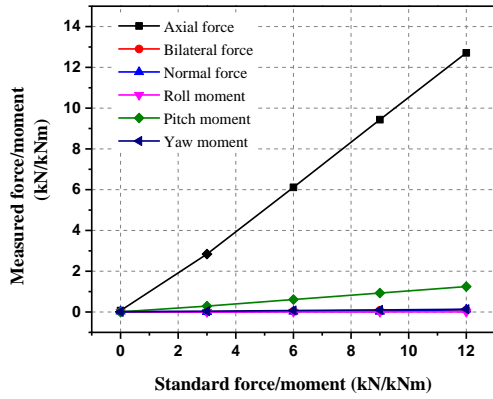
The axle force (in the x-axis) is perpendicular to the vertical hydraulic loader and parallel to the dynamometer balance plate in this test system as shown in Figure 2. The multi-range of axle force ' F_x ' is applied on point 'P1' in X-direction. The exerted force is pulling and is considered as negative. The measured output test results of the assembled dynamometer in the X-axis show 5.9% error as listed in the 3rd column of the 1st row in Table 6. The exerted axial load is partially contributing to the pitch rotation along the Y-axis, because a small support plate is fixed at the end of the top plate for the axle force and the vertical distance of this point, 'P1' is $d_{z1}=105$ mm. The linearity error is found 2.65%, the repeatability error is 0.51%, and the cross-talk error is less than 3%. The experimental analysis result of the six-component force/moment is shown in the graph (Figure 15 (a)).

Static analysis of normal/vertical force in Z-direction

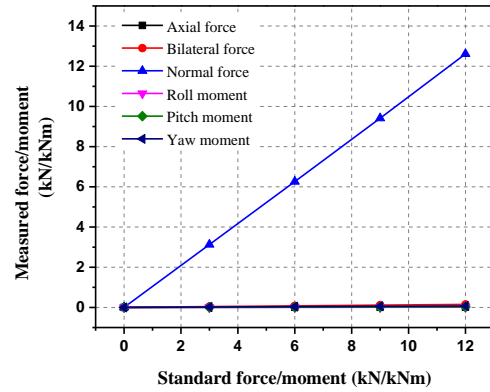
The normal force (in the Z-axis) is perpendicular to the dynamometer plate in this test system. Normal force in Z-direction is a pure normal/vertical force; therefore, it has no impact on any of the rolling, yawing, or pitching moments. The multi-range of vertical load ' F_z ' is applied on point 'P2' in the Z-direction on the centre of the upper plate of the dynamometer (Figure 7). The graph (Figure 15 (b)) shows the analyzed results of the six-component force/moment of dynamometer in Z-direction. The measured output error of the piezoelectric dynamometer in the Z-axis is 5.1%, and cross talk is under 2%.

Static analysis of the pitch moment along Y-direction

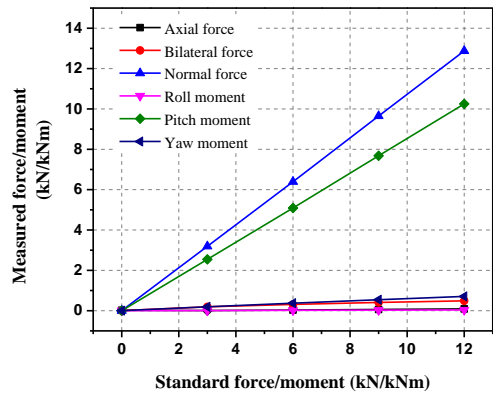
The pitch moment resembles the up and down motion of the dynamometer head considered as positive and negative respectively. The multi-load range pitch moment is applied along Y-axis on four marked points on the top of the upper plate of the dynamometer (see Figure 7). The pitch moment maximum up to 9.66 kNm is applied on point P3 in the anti-clockwise direction and on P6 in a clockwise direction. Also, a pitch moment maximum up to 4.83 kNm is applied on points P4 (in anti-clockwise) and P5 (in clockwise) directions along the Y-axis. The calibration analysis of four-moment points is discussed in Figure 15 (c-f). The measured output error of the pitch moment in the Z-axis is (min. 0.85% on P4 and max. 7.3% on P3) and cross-talk error is under 4%.



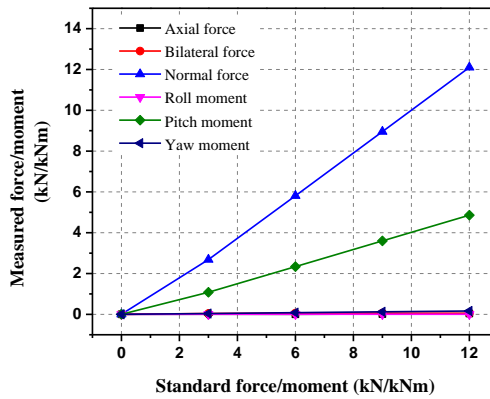
(a) Experimental analysis of axle force (F_X) on P1



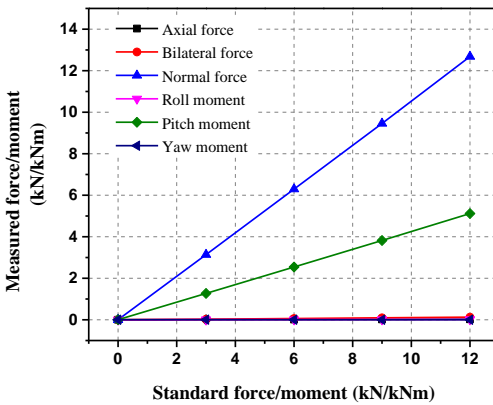
(b) Experimental analysis of normal force (F_Z) on P2



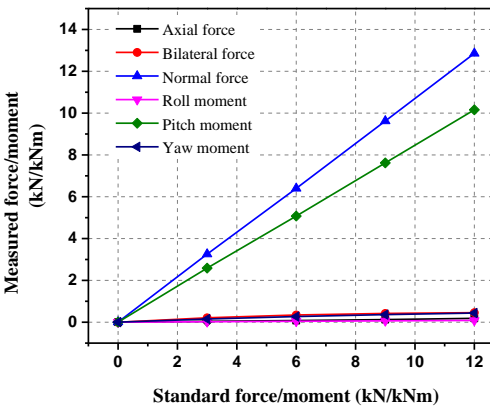
(c) Experimental analysis of anti-clockwise pitch moment (M_{Y1}) on P3



(d) Experimental analysis of anti-clockwise pitch moment (M_{Y2}) on P4



(e) Experimental analysis of clockwise pitch moment (M_{Y3}) on P5



(f) Experimental analysis of clockwise pitch moment (M_{Y4}) on P6

Figure 15. Static calibration experiment analysis (absolute values)

Dynamic calibration experiment

For performing the dynamic measurement, there is no general standard has been designed. However, dynamic calibration of the established dynamometer can be performed using two popular methods, either the power method or the excitation method [32]. Usually, the most adopted way is an impact calibration method to carry on the dynamic calibrations of six components force/torque sensors.

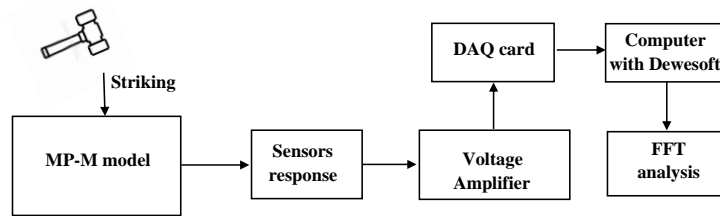


Figure 16. Schematic diagram of dynamic calibration

DeweSoft is used to conduct the fast Fourier transform (FFT) analysis and an impact load method is used to calibrate the dynamic characteristics of the piezoelectric dynamometer. The frequency response curves in three coordinates have been shown in Figure 17 and the natural frequency (ω_n) values are listed in Table 5.

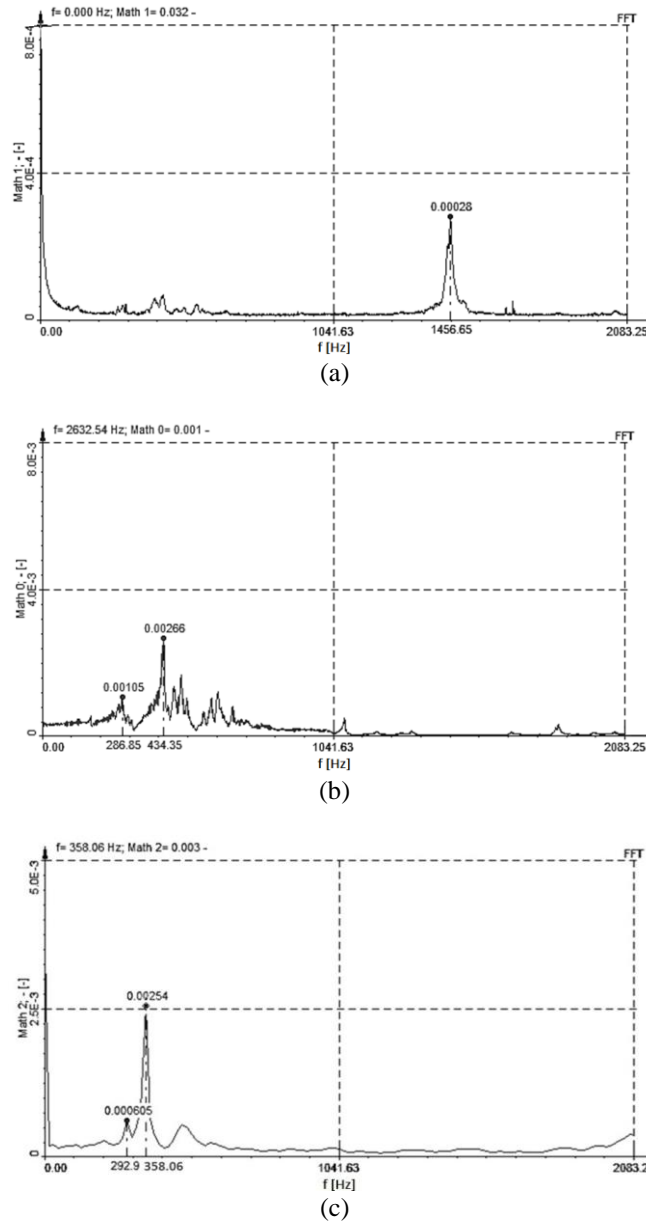


Figure 17. Curves of the frequency response characteristic: (a) curve of natural frequency characteristics in the X-direction, (b) curve of natural frequency characteristics in the Y-direction (c) curve of natural frequency characteristics in the Z-direction

Table 5. Natural frequencies ω_n (Hz) in three coordinates

Natural frequency	Axial direction ‘ F_x ’	Bilateral direction ‘ F_y ’	Vertical direction ‘ F_z ’
ω_n (Hz)	1456	434	358

The three-dimensional natural frequency of the dynamometer is shown in Table 5. . The tested dynamometer has a good response characteristic, frequency curve, and satisfies the six-dimensional force/moment measurement requirements.

DISCUSSION

The proposed piezoelectric dynamometer is analyzed both theoretically and experimentally. The theoretical simulation experiments are conducted on ANSYS using the FEM model (FEA: finite element analysis), and the calibration experiments are performed using the static calibration method and dynamic calibration method on the experimental test system. The axile force ‘ F_x ’, normal force ‘ F_z ’ maximum of 12 kN and pitch-moment ‘ M_y ’ maximum of 9.660 kNm are applied to the designed multi-points (P1-P6). The measured analysis results of both models (theoretical simulations and experimental calibration results) are in agreement with the applied standard multi-load ranges (see Table 3 and Table 6). In the experimental test system, it is hard to apply the bilateral force in the Y-direction and hence no point is designed to apply the side force.

It was complex to record the data during the calibration experiment of the dynamometer because of the multi-outputs from the mounted piezoelectric sensors. As each sensor has a three-axis output and the designed pattern includes eight tri-axial piezoelectric sensors that have a total of 24 display outputs. Therefore, in the test system, a total of 24 charge amplifiers are connected with installed load sensors. The dynamometer is calibrated by comparing the exerted known load (force/moment) with the measured output values of force/moment, and the track of their interrelationship in the similar coordinates displayed the linearity (see Figure 15). Figure 18 highlights the comparison values of linearity (%), repeatability (%), and cross-talk (%) between FEM simulation results and experimental calibration output. The experimental static calibration measurements of the multi-dimensional force-moment of the developed dynamometer are discussed in Table 6.

Table 6. Calibration experiment of multi-points piezoelectric dynamometer

Standard load		Measured force/moment (kN/kNm)					
Force (kN)	Moment (kNm)	F_x	F_y	F_z	M_x	M_y	M_z
$F_x = -12$ kN	$M_{y5} = -1.332$ kNm	-12.711	0.104	0.123	0.004	-1.245	0.135
$F_z = 12$ kN	0	0.012	0.149	12.613	0.010	0.028	0.076
$F_{z1} = 12$ kN	$M_{y1} = -9.66$ kNm	0.089	0.489	12.878	-0.035	-10.250	-0.709
$F_{z2} = 12$ kN	$M_{y2} = -4.83$ kNm	0.042	0.048	12.102	-0.003	-4.860	-0.165
$F_{z3} = 12$ kN	$M_{y3} = 4.83$ kNm	0.025	0.127	12.681	0.016	5.118	0.000
$F_{z4} = 12$ kN	$M_{y4} = 9.66$ kNm	0.184	0.455	12.856	0.085	10.158	0.438

Error (%) Comparison between FEM Simulation and Experimental Static Calibration Analysis

The linearity, repeatability, and cross-talk errors of FEM simulation experiments and experimental calibration analysis of the piezoelectric dynamometer are discussed in Figure 18.

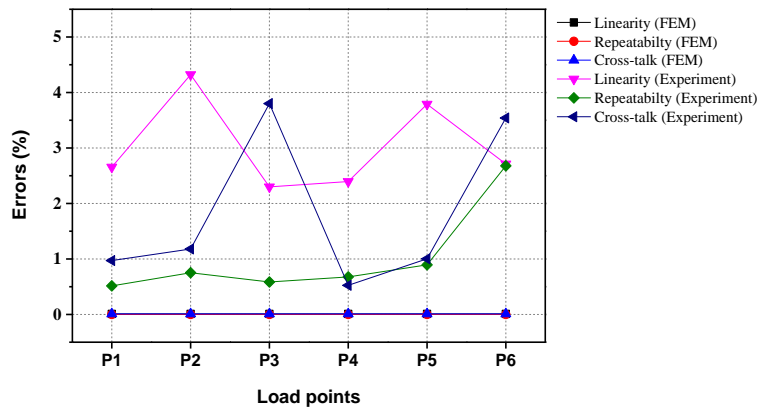


Figure 18. Error (%) comparison of FEM and Experimental analyses

The linearity, repeatability, and cross-talk errors of the axile force, normal force and pitch moments in the FEM simulation analysis are approximately zero. In the static calibration analysis, the maximum linearity error goes to 4.3% on P2 of the normal force 'F_Z' in the Z-axis and the other points have under 3.8%. The maximum repeatability error is along the Y-axis which is 2.67% of the pitch moment 'M_Y' on P6 and the repeatability error of the axile force 'F_X' and normal force 'F_Z' is less than 1%. The linearity error of multi-points P1, P3, P4, and P6 is below 3%, and P2 and P5 have under 4.5% that may be due to using a long structural model and long separation distance between installed sensors compared to most of the previous dynamometers. The repeatability error is within the acceptable range except at P6. The maximum cross-talk error is calculated on P3 and P6 of the pitch moment 'M_Y' which is found 3.8% and the cross-talk error of the other all multi-points is under 2%. The measured cross-talk error of the developed piezoelectric dynamometer is acceptable as compared with the references mentioned in Table 1.

Comparison of Measured Output (%) Results between FEM Simulation and Experimental Static Calibration Analysis

The six-component force-moment analyzed results of the FEM simulation and the experimental test system are discussed in the above tables (see Table 3 and Table 6). The comparison of measured output percent values of both analyses is listed in Table 7.

Table 7. Comparison of measured per cent values of FEM simulation analysis and Experimental calibration analysis

Multi-points	Six dimensional Force-moment	Measured output (%)	
		FEM simulation analysis	Experimental calibration analysis
P1	Axile force F _X	99.9	105.9
P2	Vertical/normal force F _Z	99.9	105.1
P3	Pitch moment M _{Y1}	100	107.3
P4	Pitch moment M _{Y2}	100	100.8
P5	Pitch moment M _{Y3}	100	105.7
P6	Pitch moment M _{Y4}	100	107.1

FEM simulation analysis values of the exerted load are approximately 99-100%, and the per cent values of static calibration experiment analysis are about 100-107%. The error difference of both analyses goes maximum up to 7% when pitch moment 'M_Y' is applied in the clockwise direction on P3 and anti-clockwise pitch moment on P6 (see Figure 5). The error output ratio of the axile force 'F_X' on P1 and normal force 'F_Z' on P2 is under 6%. Depending on the errors due to the mechanical mounting of the piezoelectric sensors in between the clamped plates of the dynamometer, assembly errors, and special instrumental errors [33], there may also be human errors or temperature errors. The measured calibration results mainly consider three variables: nonlinearity, repeatability, and cross-talk error. The maximum linearity error (4.3%) is calculated in the Z-direction when a normal force 'F_Z' is applied on P2. The maximum repeatability error (2.67%) is found along the Y-axis on P6, and the repeatability error of P1-P5 is under 1%. And the maximum cross-talk error (3.8%) occurs along the Y-axis when the pitch moment is exerted on P3, except P3 and P6 the other allocated points have their cross-talk error under 2%. The static calibration measured output of the assembled dynamometer of axile force in the X-axis is 105.9%, normal force in the Z-axis is 105.1% and the pitch moment along the Y-axis is 100.8-107.3% as shown in Table 7. The dynamometer has lower error per cent values of the axial and normal force in the X and Z-directions as compared with the pitch moment on P3 and P6 along the Y-direction.

The accuracy in the measurement of six-dimensional force/moment (F/T) is essential. The FEM simulation experiments and experimental measurement analysis proved the rationality of the piezoelectric dynamometer. The measured output of the theoretical simulations and experimental analyses is linear with the input (applied standard force/moment). The designed multi-point piezoelectric dynamometer is capable to measure the multi-axis force-moment precisely, and the measured results are discussed. Considering the fabrication technology level and using a novel pattern of piezoelectric sensors distribution with a complex experimental setup system, the design and installation of three-axis piezoelectric sensors need further improvement.

CONCLUSIONS

This research is based on the design and fabrication of the multi-point force/moment measurement piezoelectric dynamometer to perform theoretical simulation experiments and experimental calibration tests. Eight three-axis piezoelectric force sensors are designated as sensing elements and are arranged in a diagonal patterned installation to gain the spatial force information. A structural model is built and analyzed by the finite element method. To verify the numerical model, the designed piezoelectric dynamometer is manufactured, assembled and the experimental calibration tests are performed. The studied research of the designed piezoelectric dynamometer is concluded as follow:

- 1) The maximum measurement capacity of the dynamometer for a single force and for a single moment is designed maximum up to 12 kN and 9.66 kNm respectively and are applied successfully.
- 2) The FEM simulations measured results are in ranges of approximately 99-100%. The theoretical analysis of the designed multi-point piezoelectric dynamometer verified the maximum error is 0.1-0.2% in the X-axis, Z-axis, and along the Y-axis (moments).
- 3) The experimental calibration measured output is a minimum of up to 100.8% and a maximum of up to 107.3%. The experimental measurement result of axile force 'F_X' goes maximum up to 105.9% at P1, normal force 'F_Z' are maximum up to 105.1% at P2, the clockwise pitch moment 'M_Y' maximum up to 107.3% at P3 and an anti-clockwise pitch moment 'M_Y' goes a maximum of 107.1% at P6.
- 4) The difference between the measured output of the theoretical model and the experimental model is in the range of about 1-7%. The maximum difference of both models of the axial-force 'F_X', the vertical-force 'F_Z' and the pitch moments 'M_Y' is found 5.9%, 5.1% and 7.3% respectively.
- 5) The experimental calibration results are acceptable as the cross-talk is under 4%, the linearity error is maximum up to 4.3% and the repeatability error is under 3% of the six located points (P1-P6). The dynamic calibration test proved that the natural frequency (ω_n) of the dynamometer in each coordinate is greater than 0.4 kHz.

The test results showed that the fabricated piezoelectric dynamometer can accurately measure six components of force-moment of the multi-point with the multi-range of static load, and the designed dynamometer is reliable for the calibration tests. The experimental calibration test results are compared to the known rigid body FEM analysis measured results. Both models evaluate the consistency of the designed dynamometer. Furthermore, the measurement accuracy of the designed piezoelectric dynamometer can be improved with the modification in the design of the sensor assembly unit.

DECLARATION OF CONFLICTING INTERESTS

The author(s) declared no potential conflicts of interest concerning the research, authorship, and/or publication of this article.

ACKNOWLEDGMENTS

This project was supported by Aeronautical Science Foundation of China (20160163001) and the National Natural Science Foundation of China (No. 51675084).

REFERENCES

- [1] Y. Sun, Y. Liu, T. Zou, M. Jin, and H. Liu, "Design and optimization of a novel six-axis force/torque sensor for space robot," *Meas. J. Int. Meas. Confed.*, vol. 65, no. January, pp. 135–148, 2015, doi: 10.1016/j.measurement.2015.01.005.
- [2] F. Ballo, M. Gobbi, G. Mastinu, and G. Previati, "A six axis load cell for the analysis of the dynamic impact response of a hybrid III dummy," *Meas. J. Int. Meas. Confed.*, vol. 90, no. April, pp. 309–317, 2016, doi: 10.1016/j.measurement.2016.04.047.
- [3] T. P. Phan, P. C. P. Chao, J. J. Cai, Y. J. Wang, S. C. Wang, and K. Wong, "A novel 6-DOF force/torque sensor for COBOTS and its calibration method," in *Proceedings of 4th IEEE International Conference on Applied System Innovation 2018, ICASI 2018*, 2018, no. April, pp. 1228–1231, doi: 10.1109/ICASI.2018.8394511.
- [4] G. S. Kim, H. J. Shin, and J. Yoon, "Development of 6-axis force/moment sensor for a humanoid robot's intelligent foot," *Sensors Actuators, A Phys.*, vol. 141, no. 2, pp. 276–281, 2008, doi: 10.1016/j.sna.2007.08.011.
- [5] H. Akbari and A. Kazerooni, "Improving the coupling errors of a Maltese cross-beams type six-axis force/moment sensor using numerical shape-optimization technique," *Meas. J. Int. Meas. Confed.*, vol. 126, no. February, pp. 342–355, 2018, doi: 10.1016/j.measurement.2018.05.074.
- [6] Q. Xing, J. Zhang, M. Qian, Z. Jia, and B. Sun, "Design, calibration and error analysis of a piezoelectric thrust dynamometer for small thrust liquid pulsed rocket engines," *Measurement*, vol. 44, no. 2, pp. 338–344, 2011, doi: 10.1016/j.measurement.2010.10.008.
- [7] X. Jiang, K. Kim, S. Zhang, J. Johnson, and G. Salazar, "High-temperature piezoelectric sensing," *Sensors (Switzerland)*, vol. 14, no. 1, pp. 144–169, 2013, doi: 10.3390/s140100144.
- [8] S. M. Declercq, S. M. Declercq, D. R. Lazor, D. R. Lazor, D. L. Brown, and D. L. Brown, "A smart 6-DOF load cell development," in *SPIE proceedings series. Society of Photo-Optical Instrumentation Engineers*, 2002, vol. 1, no. 4753, pp. 844–853.
- [9] Z. Wang, J. Yao, Y. Xu, and Y. Zhao, "Hyperstatic analysis of a fully pre-stressed six-axis force / torque sensor," *MAMT*, vol. 57, no. August, pp. 84–94, 2012, doi: 10.1016/j.mechmachtheory.2012.07.001.
- [10] L. Qin, C. Jiang, J. Liu, and Y. Duan, "Design and calibration of a novel piezoelectric six-axis force/torque sensor," in *Seventh International Symposium on Precision Engineering Measurements and Instrumentation*, 2011, vol. 8321, pp. 83210G-83210G-9, doi: 10.1117/12.903717.

- [11] C. Yuan *et al.*, “Development and evaluation of a compact 6-axis force/moment sensor with a serial structure for the humanoid robot foot,” *Meas. J. Int. Meas. Confed.*, vol. 70, no. March, pp. 110–122, 2015, doi: 10.1016/j.measurement.2015.03.027.
- [12] Z. N. Brimhall, N. Divitotawela, J. P. Atkinson, D. L. Kirk, and H. G. Peebles, “Design and validation of a six degree of freedom rocket motor thrust stand,” in *44th AIAA/ASME/SAE/ASEE Joint Propulsion Conference & Exhibit*, 2008, no. July, pp. 1–7, doi: <https://doi.org/10.2514/6.2008-5051>.
- [13] F. Ballo, M. Gobbi, G. Mastinu, and G. Previati, “Advances in force and moments measurements by an innovative six-axis load cell,” *Exp. Mech.*, vol. 54, no. 4, pp. 571–592, 2014, doi: 10.1007/s11340-013-9824-4.
- [14] Z. Jia, Y. Gao, Z. Ren, S. Gao, and Y. Shang, “Design and calibration method for a novel six-component piezoelectric balance,” *Proc. Inst. Mech. Eng. Part C J. Mech. Eng. Sci.*, vol. 227, no. 8, pp. 1841–1852, 2013, doi: 10.1177/0954406213499285.
- [15] Z. Y. Jia, S. Lin, and W. Liu, “Measurement method of six-axis load sharing based on the Stewart platform,” *Meas. J. Int. Meas. Confed.*, vol. 43, no. 3, pp. 329–335, 2010, doi: 10.1016/j.measurement.2009.11.005.
- [16] Y. J. Li, J. Zhang, Z. Y. Jia, M. Qian, and H. Li, “Research on force-sensing element’s spatial arrangement of piezoelectric six-component force/torque sensor,” *Mech. Syst. Signal Process.*, vol. 23, no. 8, pp. 2687–2698, 2009, doi: 10.1016/j.ymsp.2009.05.014.
- [17] Y. jun Li, C. Yang, G. cong Wang, H. Zhang, H. yong Cui, and Y. liang Zhang, “Research on the parallel load sharing principle of a novel self-decoupled piezoelectric six-dimensional force sensor,” *ISA Trans.*, vol. 70, no. July, pp. 447–457, 2017, doi: 10.1016/j.isatra.2017.07.008.
- [18] Z. Jia, L. Jin, W. Liu, and Z. Ren, “A novel strategy to eliminate the influence of water adsorption on quartz surfaces on piezoelectric dynamometers,” *Sensors (Switzerland)*, vol. 16, no. 7, pp. 1–10, 2016, doi: 10.3390/s16071060.
- [19] P. Baki, G. Székely, and G. Kósa, “Design and characterization of a novel, robust, tri-axial force sensor,” *Sensors Actuators, A Phys.*, vol. 192, no. December, pp. 101–110, 2013, doi: 10.1016/j.sna.2012.11.035.
- [20] J. Schleichert, I. Rahneberg, and T. Fröhlich, “Calibration of a Novel Six-Degree-of-Freedom Force/Torque Measurement System,” *Int. J. Mod. Phys. Conf. Ser.*, vol. 24, pp. 1360017 (1–9), 2013, doi: 10.1142/s2010194513600173.
- [21] T. A. Dwarakanath and D. Venkatesh, “Simply supported , ‘ Joint less ’ parallel mechanism based force – torque sensor,” *Mechatronics*, vol. 16, no. March, pp. 565–575, 2006, doi: 10.1016/j.mechatronics.2006.03.013.
- [22] M. K. Kang, S. Lee, and J. H. Kim, “Shape optimization of a mechanically decoupled six-axis force/torque sensor,” *Sensors Actuators, A Phys.*, vol. 209, no. January, pp. 41–51, 2014, doi: 10.1016/j.sna.2014.01.001.
- [23] M. Gobbi, G. Previati, P. Guarneri, and G. Mastinu, “A new six-axis load cell . Part II : Error analysis , construction and experimental assessment of performances,” *Exp. Mech.*, vol. 51, no. May, pp. 389–399, 2011, doi: 10.1007/s11340-010-9350-6.
- [24] Z. H. Zhang, B. Y. Sun, M. Qian, J. Zhang, Y. H. Shi, and X. Zhou, “An investigation of the tertiary coupling effect under the longitudinal mode of a piezoelectric crystal,” *Proc. Inst. Mech. Eng. Part C J. Mech. Eng. Sci.*, vol. 223, no. 8, pp. 1777–1785, 2009, doi: 10.1243/09544062JMES1247.
- [25] W. Liu, Y. J. Li, Z. Y. Jia, J. Zhang, and M. Qian, “Research on parallel load sharing principle of piezoelectric six-dimensional heavy force/torque sensor,” *Mech. Syst. Signal Process.*, vol. 25, no. 1, pp. 331–343, 2011, doi: 10.1016/j.ymsp.2010.09.008.
- [26] Q. Xing *et al.*, “Thrust stand for low-thrust liquid pulsed rocket engines Thrust stand for low-thrust liquid pulsed rocket engines,” *Rev. Sci. Instrum.*, vol. 81, pp. 095102 (1–8), 2010, doi: 10.1063/1.3481788.
- [27] Z. Ren, S. Gao, Z. Jia, and Y. Shang, “Piezoelectric sensor of control surface hinge moment,” *Sensors & Transducers*, vol. 152, no. 5, pp. 11–17, 2013, Retrieved from https://www.sensorsportal.com/HTML/ST_Journal.htm.
- [28] A. Cigada, M. Falco, and A. Zasso, “Development of new systems to measure the aerodynamic forces on section models in wind tunnel testing,” *J. Wind Eng. Ind. Aerodyn.*, vol. 89, pp. 725–746, 2001, doi: [doi.org/10.1016/S0167-6105\(01\)00075-7](https://doi.org/10.1016/S0167-6105(01)00075-7).
- [29] J. Liu, M. Li, L. Qin, and J. Liu, “Active design method for the static characteristics of a piezoelectric six-axis force/torque sensor,” *Sensors (Switzerland)*, vol. 14, no. 1, pp. 659–671, 2014, doi: 10.3390/s140100659.
- [30] N. Ulbrich, “Combined Load Diagram for a Wind Tunnel Strain–Gage Balance,” in *27th AIAA Aerodynamics Measurement and Ground Testing Conference*, 2010, no. July, pp. 1–18, doi: 10.2514/6.2010-4203.
- [31] J. Zhang, J. Shao, Z. Ren, B. Wang, H. Shao, and Z. Jia, “Research on dimension coupling of piezoelectric three-component force unit based on sensor assembly error,” *Adv. Mech. Eng.*, vol. 11, no. 5, pp. 1–11, 2019, doi: 10.1177/1687814019846291.
- [32] Y. Zhang, B. Guan, and H. Tam, “Characteristics of the distributed Bragg reflector fiber laser sensor for lateral force measurement,” *Opt. Commun.*, vol. 281, no. May, pp. 4619–4622, 2008, doi: 10.1016/j.optcom.2008.05.039.
- [33] I. Korobiichuk, “Analysis of errors of piezoelectric sensors used in weapon stabilizers,” *Metrol. Meas. Syst.*, vol. 24, no. 1, pp. 91–100, 2017, doi: 10.1515/mms-2017-0001.